# Journal of Materials Chemistry C

Accepted Manuscript

This article can be cited before page numbers have been issued, to do this please use: S. KUMAR, C. An, S. Sahoo, R. Griniene, D. Volyniuk, J. V. Grazulevicius, S. Grigalevicius and J. Jou, *J. Mater. Chem. C*, 2017, DOI: 10.1039/C7TC03049E.




ROYAL SOCIETY OF CHEMISTRY

rsc.li/materials-c

# Solution-processable naphthalene and phenyl substituted carbazole core based hole transporting materials for efficient organic light-emitting diodes

Sudhir Kumar[a,b], Chih-Chia An[a], Snehasis Sahoo[a], R. Griniene[c], D. Volyniuk[c], Juozas V. Grazulevicius[c], Saulius Grigalevicius[c,*], Jwo-Huei Jou[a,*]

[a]Department of Materials Science and Engineering, National Tsing-Hua University, No.101, Kung-Fu Rd. Hsin-Chu 30013 Taiwan, R.O.C.

[b]Institute for Chemical and Bioengineering, ETH Zürich, Vladimir Prelog Web 1, 8093 Zürich, Switzerland.

[c]Department of Polymer Chemistry and Technology, Kaunas University of Technology, Radvilenu plentas 19, LT50254, Kaunas, Lithuania.



## Abstract

Solution-processable molecular hole transporting material (HTM) is extremely crucial in order to realize the low cost, high throughput, and roll-to-roll fabrication of large area organic light emitting diodes for display and lighting applications. In this report, a series of naphthalene and phenyl substituted carbazole core based HTMs, 3-(1-naphthyl)-9-(2-phenylvinyl)carbazole (NPVCz), 3,6-di-(1-naphthyl)-9-phenylvinylcarbazole (DNPVCz), and 3,6-diphenyl-9-(2-phenylvinyl)carbazole (DPPVCz) are successfully synthesized and characterized. The synthesized HTMs possess excellent solubility in common organic solvents. By using a fluorescent *tris*(8-hydroxyquinolinato)aluminium emitter, we demonstrate an enhancement of 135%, from 1.7 to 4.5 cd $A^{-1}$, in current efficiency of organic light emitting diode (OLED) by replacing the conventional HTM, *N*,*N*'-di(1-naphthyl)-*N*,*N*'-diphenyl-(1,1'-biphenyl)-4,4'-diamine (NPB), with the NPVCz counterpart. Moreover, the current efficiency of a conventional *tris*[2-phenylpyridinato-C2,*N*]iridium(III) based phosphorescent green OLED device increases from 46.4 to 66.2 cd $m^{-2}$ by substituting the NPB from the NPVCz. These findings suggest that such type of solution-processable molecular HTMs will be promising contender for high efficiency OLED devices.

## 1. Introduction

Organic light emitting diodes (OLEDs) have attracted the great attention because of their extensive applications in high quality displays and lightings.[1,2] At the present time numerous type of portable display devices and a few large size OLED televisions have already been in

View Article Online
DOI: 10.1039/C7TC03049E





the market.[2,3] At present, almost every single commercial OLED product is fabricated by vacuum deposition because of its superlative features, such as precise layer thickness control, high efficiency, and easy multilayer deposition in the intricate devices, which are highly expensive because of low throughput and huge materials wastage.[4] To make the resultant products commercially profitable and large-area roll-to-roll fabrication, solution-processable OLEDs with higher efficiencies are extremely demanded.[5-9]

Nowadays, it is well established that carrier transporting materials are crucial to enable a balance carrier, electron and hole, transport from the counter electrodes (cathode and anode). Moreover, these layers should facilitate a confinement of injected carriers within the emissive layer to realize a high efficiency OLED devices.[10-11] Numerous type of high triplet energy electron transporting materials have been reported, while only a few hole transporting materials (HTMs) have been realized for OLED devices.[12] A high triplet energy HTM with high mobility and can effectively increase the carrier injection balance and exciton confinement, respectively. Typically, arylamines,[13,14] carbazoles,[15-18] carbazole-arylamine hybrids,[19] and tolylamino cyclohexane[20] derivatives have been extensively studied as HTM in OLEDs because of their high hole mobility, electron confining ability, and amorphous film forming property. Amongst, arylamine derivatives, such as *N*,*N*'-diphenyl-*N*,*N*'-bis(1-naphthyl)-(1,1'-biphenyl)-4,4'-diamine (NPB), *N*,*N*'-bis(3-methylphenyl)-*N*,*N*'-bis(phenyl) benzidine (TPD), and 1,1-bis((di-4-tolylamino)phenyl)cyclohexane (TAPC), have been widely used as HTMs because of their high hole mobility and ease of thermal evaporation.[13-15,21,22] Though, their poor film forming ability, low morphological stability, and ease of crystallization at room temperature caused the poor device efficiency or device failure in solution-process.[14,23]

On the other hand, carbazole derivatives, such as tris(4-carbazoyl-9-ylphenyl)amine (TCTA),[24] 3,6-bis(4-vinylphenyl)-9-ethylcarbazole (VPEC),[25] and tris(4-carbazole)triphenyl

View Article Online
DOI: 10.1039/C7TC03049E



amine,[26] have been also studied as the HTM due to their rational hole mobility, high triplet energy, amorphous film forming ability, and high thermal stability. Numerous solution-processable long chain polymeric, and oligomeric type HTMs have been reported, while they exhibited a poor device efficiency.[27-32] However, only a few dendritic HTMs have been investigated in OLED devices, and they have exhibited relatively higher efficiency than that of polymer counterparts. For example, Moonsin et al.[33] reported a maximum current efficiency ($\eta_{CE}$) of 4.45 cd $A^{-1}$ as a dendritic carbazole derivative, 3',6'-bis[3,6-bis(carbazole-9-yl)carbazole-9-yl]-bis[9-(2-ethylhexyl) carbazole-3,6-diyl, was spin-coated between the hole injection layer of poly(3,4-ethylenedioxythiopene):poly(styrenesulfonate) (PEDOT:PSS) and an emissive/electron transporting layer of tris(8-hydroxyquinolinato)aluminium ($Alq_3$). Usluer et al.[34] reported a maximum $\eta_{CE}$ of 7.7 cd $A^{-1}$ by employing a newly synthesized fluorene-carbazole dendrimer based HTM between the PEDOT:PSS and $Alq_3$ layers. Prachumrak et al.[35] designed and synthesized a series of carbazole dendrimers based HTMs for OLEDs. The resultant device exhibited a maximum $\eta_{CE}$ of 5.11 cd $A^{-1}$ by using a five carbazole units based HTM, 3,6-bis[3',6'-bis(3",6"-di-*tert*-butylcarbazol-*N*"-yl)carbazol-*N*'-yl]-*N*-dodecylcarbazole (G3C). Recently, solution-process feasible molecular HTMs attracted a considerable attention in OLEDs over long-chain polymer or complex dendrimer counterparts because of their easy synthesis, high degree of purity, defect free structure, and higher hole mobility.[36,37] Most importantly, molecular HTMs based OLEDs have shown excellent reproducibility because of smaller chain entanglement than that of the long chain polymer counterparts.[37] The design of wet-process feasible molecular HTM is highly challenging because they must have to offer a high solubility in common organic solvents with excellent film forming property, film integrity, and amorphous film morphology. In the past years, a few solution-processable molecular HTMs have been reported, for example, Wu et al.[38] synthesized a tri-carbazole functionalized fluorenyl core based compound 2,4,7-tri[2-

(9-hexylcarbazole)-ethynyl]-9,9-dihexyl fluorene. The resultant multilayer OLED device exhibited a maximum $\eta_{CE}$ of 3.2 cd $A^{-1}$. Thaengthong et al.[39] synthesized a carbazole-type amorphous HTM of 3′,6′-bis(carbazol-9-yl)-bis[9-(2-ethylhexyl)carbazol-3,6-diyl], and employed in a double layer OLED device. Hence, it is worthy to devise a solution-processable small molecular type HTM for OLED devices.

In this study, we demonstrate a series of naphthyl and phenyl substituted 9-(2-phenylvinyl) carbazole type HTMs, 3,6-diphenyl-9-(2-phenylvinyl)carbazole (DPPVCz), 3-(1-naphthyl)-9-(2-phenylvinyl)carbazole (NPVCz), and 3,6-di-(1-naphthyl)-9-phenylvinyl carbazole (DNPVCz). These HTMs exhibit excellent solubility in common organic solvents and robust thermal stability. Taking double layer fluorescent green device for example, at 1000 cd $m^{-2}$, the $\eta_{CE}$ is enhanced from 1.7 to 4.5 cd $A^{-1}$ and a power efficiency ($\eta_{PE}$) from 1.7 to 2.6 lm $W^{-1}$, as NPB is replaced by NPVCz. Moreover, conventional *tris*[2-phenylpyridinato-C2,*N*]iridium(III), $Ir(ppy)_3$, emitter based green phosphorescent device shows a maximum $\eta_{CE}$ of 66.2 cd $A^{-1}$ ($\eta_{PE}$ =70.0 lm $W^{-1}$ and external quantum efficiency, $\eta_{ext}$ = 18.3%) with solution-processable NPVCz, and improves by almost 40% compared to the OLED based on the NPB. The high device efficiency is attributed to rational hole mobility and effective electron confinement. Moreover, the phosphorescent device architecture enabling therein an electron trap to facilitate the injection of the minor carriers against that of a hole, leading to a more balance carrier injection.

## 2. Result and discussion

### 2.1 Synthesis

The synthesis of naphthyl and phenyl substituted 9-(2-phenylvinyl) carbazole derivatives, NPVCz, DNPVCz, and DPPVCz, was carried out by multi-step synthetic routes shown in **Scheme 1**. The key starting materials 3-iodo-*9H*-carbazole (**2**) and 3,6-di-iodo-*9H*-carbazole (**3**) were synthesized from commercially available *9H*-carbazole (**1**) by Tucker iodination

with KI/$KIO_3$ in acetic acid.[40] The 3-iodo-9-(2-phenylvinyl) carbazole (**4**) and 3,6-di-iodo-9-(2-phenylvinyl)carbazole (**5**) were synthesized, respectively, by condensation reaction of the iododerivatives **2** and **3** with an excess of 2-phenylacetaldehyde under acidic conditions in the presence of (±)-camphor-10-sulfonic acid. The naphthyl substituted carbazole derivatives NPVCz and DNPVCz were obtained by Suzuki coupling reaction of the compounds **4** and **5**, correspondingly, with an excess of 1-naphtalene boronic acid. On the other hand, the compound DPPVCz was synthesized by Suzuki coupling reaction of the compound **5** with an excess of phenyl boronic acid. Molecular structures of all compounds were characterized by 1H NMR, IR, and HRMS techniques (see spectra in **Fig. S1** to **S5**).

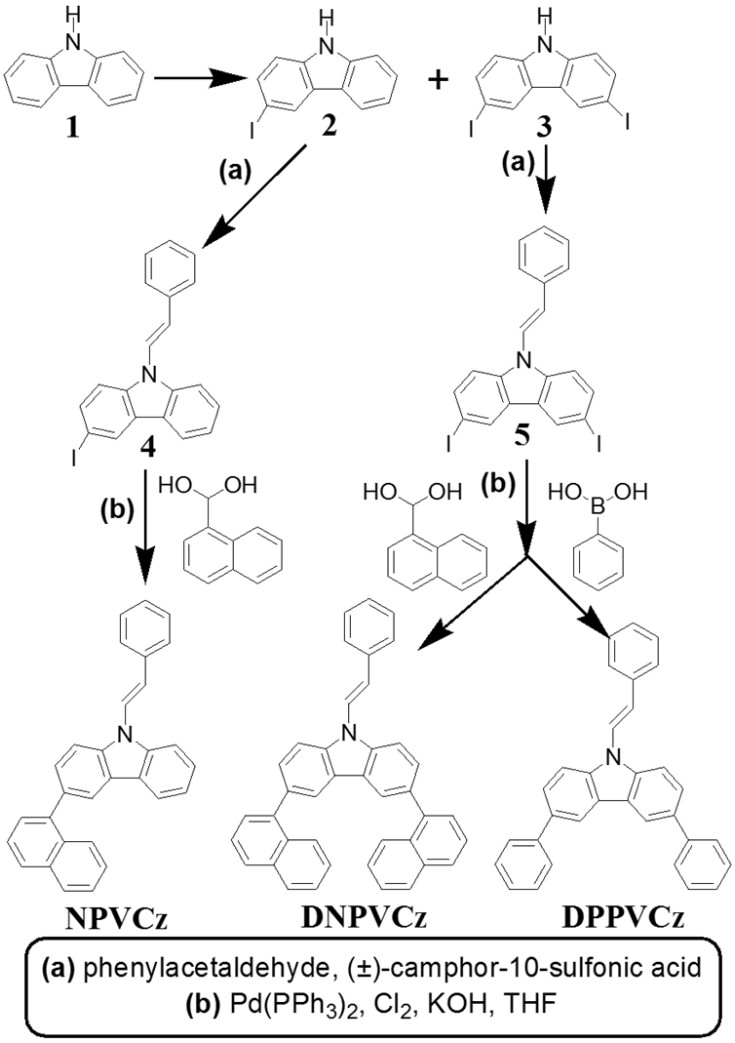


**Scheme 1.** Schematic illustration of the synthesis of the naphthyl and phenyl substituted 9-(2-phenylvinyl) carbazole based hole transporting materials (HTMs), NPVCz, DNPVCz, and DPPVCz.

View Article Online
DOI: 10.1039/C7TC03049E





## 2.2 Photophysical properties

As shown in **Fig. 1**, the ultraviolet-visible (UV-vis) and photoluminescence (PL) spectra of the compounds NPVCz, DNPVCz, and DPPVCz were measured in tetrahydrofuran (THF) at room temperature. The optical band gaps ($E_g$) were estimated from intersections of the absorption spectra. The compounds NPVCz, DNPVCz, and DPPVCz show the $E_g$ of 3.28 eV, 3.32 eV, and 3.29 eV, respectively. The triplet-energies ($E_T$) were calculated from the first triplet emission peak of the low temperature PL spectrum measured in cryogenic medium (liquid $N_2$) at 77K (**Fig. S6**), which exhibit the $E_T$ of 3.09 eV, 2.84 eV and 2.69 eV, respectively, for NPVCz, DNPVCz and DPPVCz.

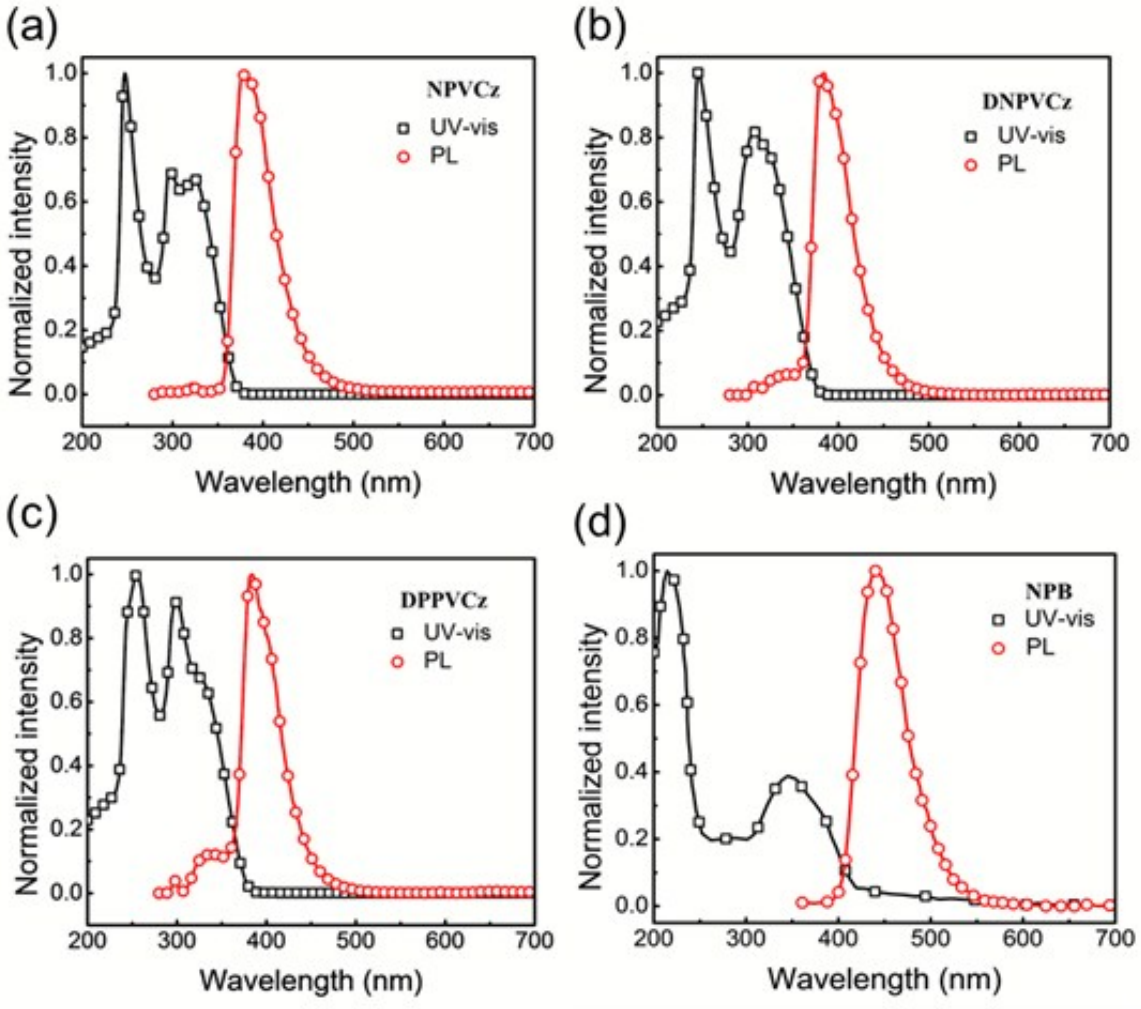


**Figure 1.** The ultraviolet-visible (UV-vis) and photoluminescence (PL) spectra of the naphthalene and phenyl substituted carbazole core based HTMs, (a) NPVCz, (b) DNPVCz, (c) DPPVCz, and (d) NPB. All the data were measured by dissolving the HTMs in THF.

View Article Online
DOI: 10.1039/C7TC03049E

**Table 1**. Photophysical, electrochemical, and thermal characteristics of the novel hole transporting materials.

| HTM | $\lambda_{abs}$ (nm) | $\lambda_{em}$ (nm) | HOMO[a)] (eV) | LUMO[a)] (eV) | $E_g$ (eV) | $E_T$ (eV) | $T_d$[b)] (°C) | $T_m$ [c)] (°C) | $T_g$[d)] (°C) | $\mu_h$ [e)] ($cm^2.V^{-1}.s^{-1}$) |
|---|---|---|---|---|---|---|---|---|---|---|
| NPVCz | 326, 298, 247 | 381 | 5.27 | 2.12 | 3.15 | 3.09 | 379 | 120 | 57 | $2.4\times10^{-4}$ |
| DNPVCz | 308, 245 | 384 | 5.31 | 2.21 | 3.10 | 2.82 | 461 | 265 | 107 | $1.5\times10^{-4}$ |
| DPPVCz | 299, 255 | 384 | 4.93 | 1.82 | 3.11 | 2.69 | 360 | 184 | 55 | $3.5\times10^{-5}$ |
| NPB | 345, 215 | 450 | 5.50* | 2.40* | 3.10* | 2.30* | 350 | 280[15a] | 95[15a] | $4.1\times10^{-4}$ [15b] |

[a)]HOMO and LUMO values were measured by cyclic voltammetry method. Semi-oxidation potential ($E_{1/2}^{ox}$) could be calculated from ($E_{p1}+E_{p2}$)/(2-0.48). Where 0.48 is correction value obtained by the oxidation system was added $Fc^+/Fc$ as the internal standard, and $E_{HOMO} = -(E_{1/2}^{ox} + 4.8)$. $E_{LUMO} = (E_{HOMO} - E_g)$. [b)]decomposition temperature. [c)]melting temperature. [d)]glass-transition temperature. [e)]hole mobility. Ref. 15.

### 2.3 Electrochemical properties

The electrochemical properties of all three HTMs were characterized by cyclic voltammetry. The highest occupied molecular orbital (HOMO) energy levels were calculated by using the oxidation potentials, which were estimated from the cyclic voltammograms (**Fig. 2**). The resultant HOMO levels are -5.27, -5.31 and -4.93 eV for the NPVCz, DNPVCz, and DPPVCz, respectively. The lowest unoccupied molecular orbital (LUMO) energy levels of the HTMs were calculated from HOMO energy level and optical energy band gap ($E_g$), which are -1.99, -1.99 and -1.64 eV, respectively. The determined oxidation potentials ($E_{1/2}^{ox}$), energy bandgaps, HOMO and LUMO values are listed in **Table 1**.

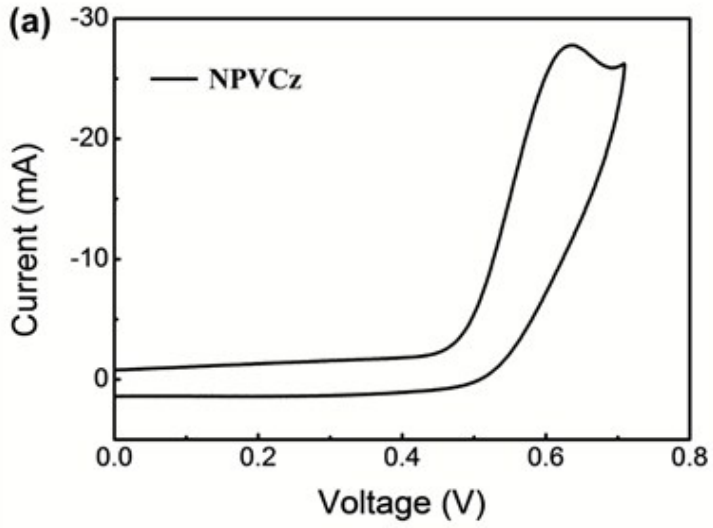

View Article Online
DOI: 10.1039/C7TC03049E



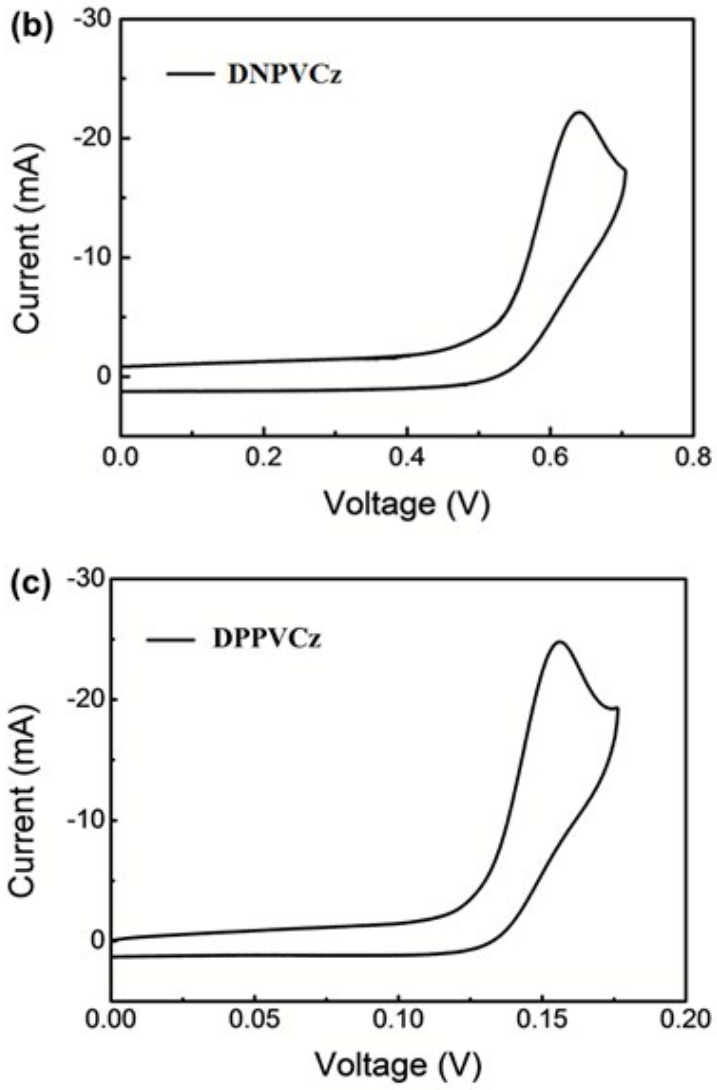


**Figure 2.** Cyclic voltammograms of the compounds (a) NPVCz, (b) DNPVCz, and (c) DPPVCz.

### 2.4 Thermal and morphological properties

The thermal behavior of the compounds DPPVCz, NPVCz, and DNPVCz was characterized by using differential scanning calorimetry (DSC) and thermogravimetric analysis (TGA) techniques. As shown in **Fig. S7**, the melting temperatures ($T_m$) of the compounds are ranged from 120 $^oC$ to 265 $^oC$, and the glass transition temperatures ($T_g$) from 55 $^oC$ to 107 $^oC$, respectively. The thermal behavior of the HTMs is strongly depended on the type of substituents (phenyl and naphthalene) and the number of substituent units.

View Article Online
DOI: 10.1039/C7TC03049E



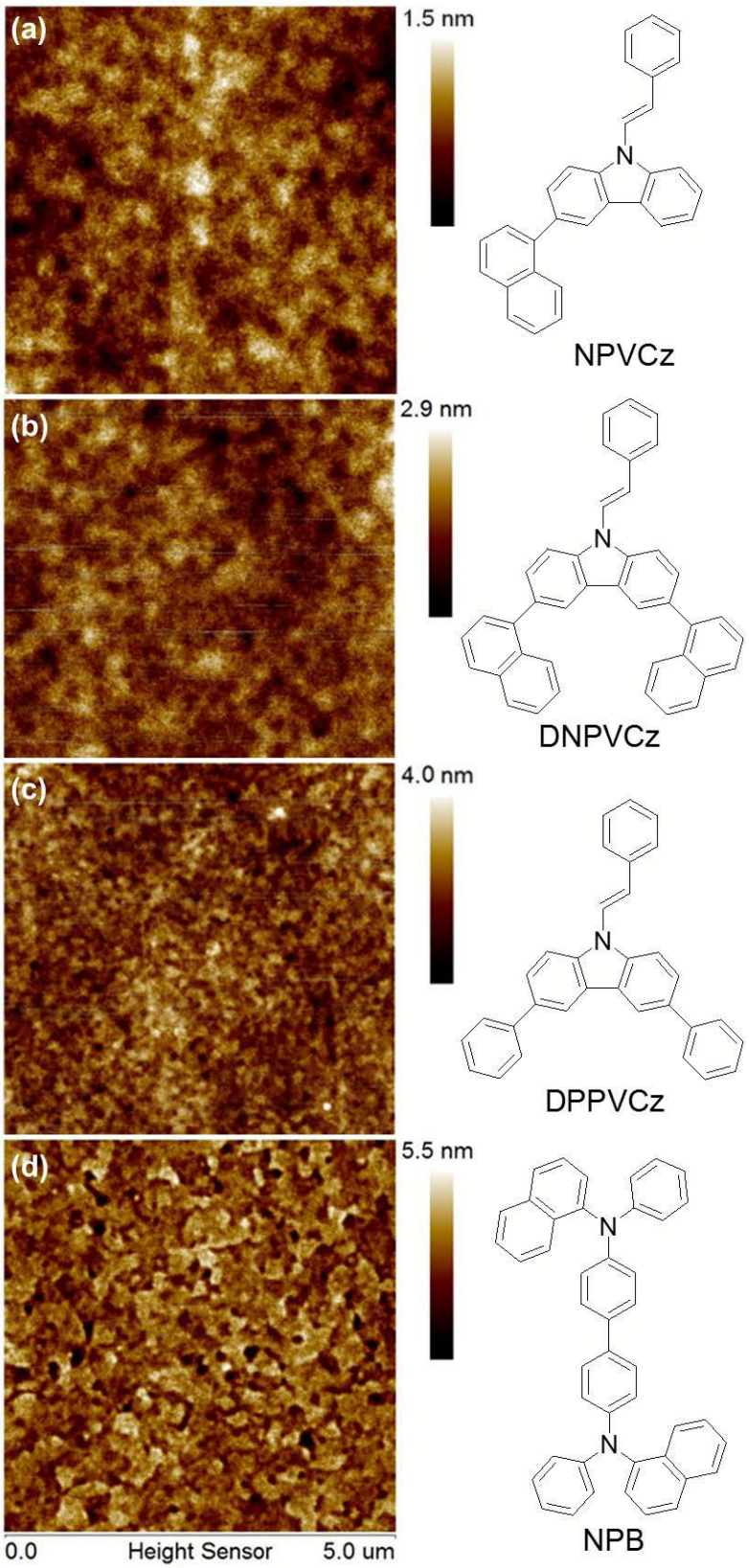


**Figure 3.** Surface morphologies of the spin-coated films and molecular structures of the novel HTMs (a) NPVCz, (b) DNPVCz, and (c) DPPVCz, and a typical HTM (d) NPB. All the films were spin-coated from THF solutions onto the PEDOT:PSS layer as employed in devices.

As shown in **Table 1**, two phenyl groups substituted carbazole core based compound DPPVCz compound shows the lowest $T_g$ value of 55 $^oC$, while the $T_g$ increases to 57 $^oC$ for the asymmetric NPVCz compound with one naphthalene unit. The $T_g$ of compound extensively increases from 57 $^oC$ to 107 $^oC$ for the DNPVCz as an additional naphthalene unit was introduced on to the carbazole core of the NPVCz compound. As shown in **Fig. S8**, the compounds DPPVCz and NPVCz, DNPVCz exhibit a thermal decomposition temperatures ($T_d$) of 360 $^oC$, 379 $^oC$, and 461 $^oC$, respectively, corresponding to a 5% weight loss. Amongst, the highest $T_d$ of the DNPVCz may arise because of the fused molecular structure and two naphthalene substituents. The robust thermal characteristic of compounds may facilitate the excellent film integrity under electrical excitation.[41] Because an organic material is less vulnerable to heat and forms stable amorphous film with increasing $T_g$. In contrast, the low $T_g$ organic compounds easily crystallize that affects film homogeneity, and crystal boundaries raise the electrical resistance to the carriers. Therefore, high $T_g$ materials result into better film integrity and leads to better device performance.[41]

As shown in **Fig. 3**, the surface morphologies of the spin-coated films of the HTMs were characterized by the atomic-force microscopy (AFM). The resultant root-mean-square (rms) surface roughness values are 0.41, 0.38, 0.62, and 0.76 nm for the NPVCz, DNPVCz, DPPVCz, and NPB, respectively. All the spin-coated films exhibit smooth surface topologies without any crystallization. The bi-naphthyl units substituted carbazole core based compound, DNPVCz, shows relatively low film roughness. It has been found that the newly synthesized carbazole core based HTMs, NPVCz, DNPVCz, DPPVCz, exhibit relatively much smoother film morphologies than that of typical NPB counterpart.

### 2.5 Hole mobility

The hole mobility ($\mu_h$) of the compounds DPPVCz NPVCz, and DNPVCz was measured by the time-of-flight (TOF) technique.[42,43] The $\mu_h$ was calculated by the formula of $\mu_h$ =

View Article Online
DOI: 10.1039/C7TC03049E

$d^2/(V.t_T)$, where $d$ is the layer thickness of the compounds, V applied bias, and $t_T$ carrier transit time.[44,45] The $\mu_h$ determined for the carbazole core based HTMs is shown as a function of the square root of electric field ($E^{1/2}$) in **Fig. 4** (see transient photocurrent curves in **Fig. S9**). The $\mu_h$ of the compounds DPPVCz, NPVCz and DNPVCz are ranged from $3.5\times10^{-5}$ to $2.4\times10^{-4}$ $cm^2/V\cdot s$, as shown in **Table 1**.

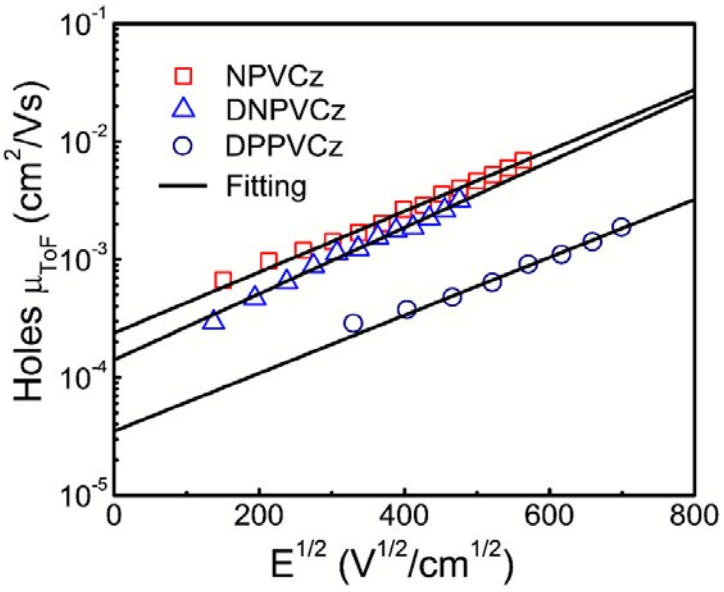


**Figure 4.** The hole mobility of the HTMs, NPVCz, DNPVCz and DPPVCz, as a function of the square root of electric field.

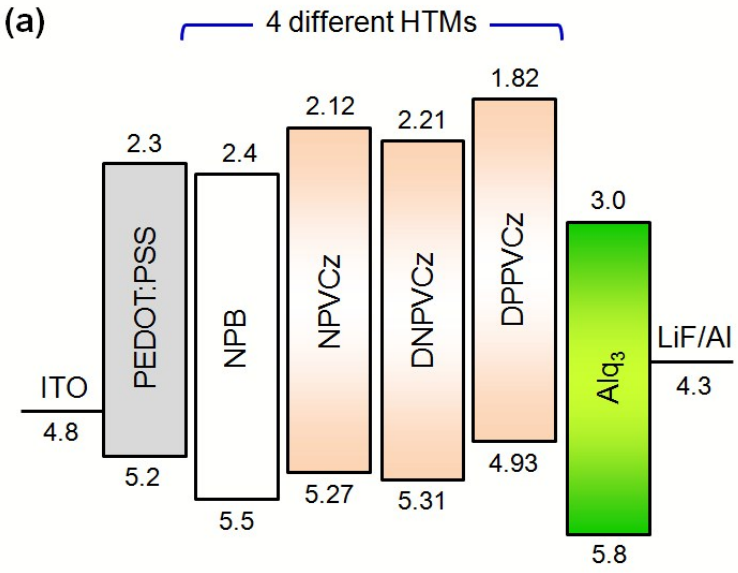

View Article Online
DOI: 10.1039/C7TC03049E

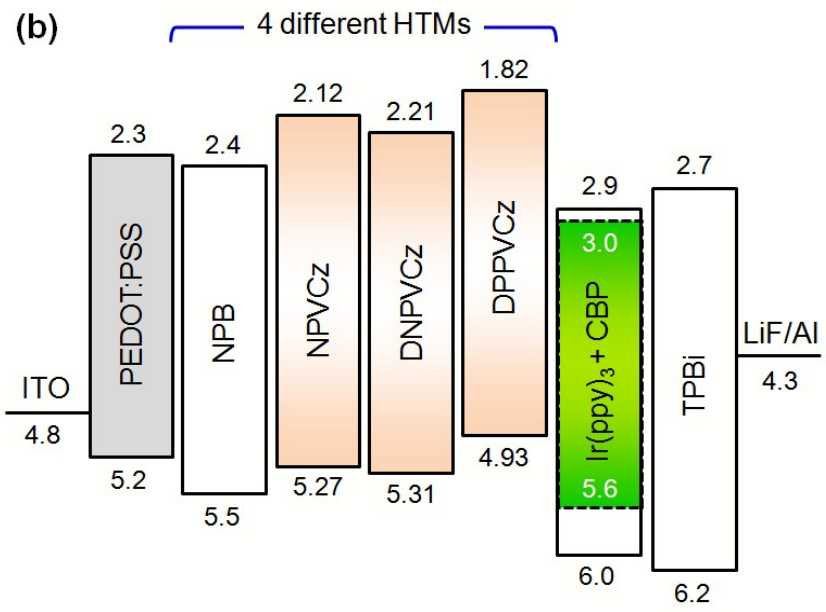


**Figure 5.** Schematic diagram of the energy levels of the (a) fluorescent and (b) phosphorescent OLED devices containing the spin-coated films of four different HTMs, NPVCz, DNPVCz, DPPVCz, and NPB.

### 2.6 Electroluminescent characteristics

**Fig. 5a** shows the schematic energy-level diagrams of the OLED devices studied herein. Taking the fluorescent green OLED device for example, the fabrication process included firstly spin-coating an aqueous solution of PEDOT:PSS at 4000 rpm for 20 s to form a hole-injection layer (HIL) on a pre-cleaned ITO anode. Before spin-coating the following hole transporting layer (HTL), the solution was prepared by dissolving three different concentrations 2, 4 and 6 mg $ml^{-1}$ of the HTMs (NPVCz, DNPVCz, and DPPVCz) in tetrahydrofuran at room-temperature with stirring for 0.5 h. The resulting solution was then spin-coated at 2500 rpm for 20 s under nitrogen. Followed were the depositions of the emission layer/electron-transporting layer $Alq_3$, the electron injection layer LiF, and the cathode Al, by thermal evaporation in a vacuum chamber at a vacuum level of less than $5 \times 10^{-6}$ Torr. A standard device was also fabricated for comparison by using NPB as HTL. As shown in **Fig. 5b**, the phosphorescent green device contain a 32 nm HIL of PEDOT:PSS, which was spin-coated on a pre-cleaned ITO coated glass substrate. Subsequently, a 25 nm

View Article Online
DOI: 10.1039/C7TC03049E

HTM and 20 nm EML were spin-coated on the PEDOT:PSS coated substrate. Finally, a 35 nm ETL of TPBi, a 1 nm EIL of LiF, and a 100 nm Al cathode, were deposited by the thermal evaporation.

**Table 2.** Electroluminescence (EL) characteristics of double layer fluorescent OLED devices by using newly synthesized carbazole derivatives, NPVCz, DPPVCz, and DNPVCz, and a typical NPB as hole transporting layer.

| HTL | $V_{driv}$ (V) | $\eta_{PE}$ (lm/W) | $\eta_{CE}$ (cd/A) | 1931 $CIE_{x,y}$ Coordinates | Maximum luminance ($cd/m^2$) |
|---|---|---|---|---|---|
| | @ 100 /1,000 $cd/m^2$ | | | | |
| NPB | 3.6/5.4 | 2.4/1.7 | 2.7/1.7 | (0.32, 0.52)/(0.32, 052) | 4218 |
| NPVCz | 3.9/ 5.4 | 3.3/ 2.6 | 4.1/ 4.5 | (0.33, 0.54)/ (0.33, 0.54) | 10360 |
| DNPVCz | 3.8/ 5.3 | 3.0/ 2.4 | 3.7/ 4.0 | (0.34, 0.54)/(0.34, 0.54) | 4748 |
| DPPVCz | 4.1/5.9 | 2.0/1.7 | 2.6/3.1 | (0.34, 0.55)/ (0.34, 0.55) | 5829 |

### *2.6.1. Fluorescent OLED devices*

The current density (*J*), luminance (*L*), $\eta_{PE}$, and $\eta_{CE}$ of two layer green fluorescent OLEDs are presented in **Fig. 6a**. All the three HTMs based devices also show higher efficiencies and luminance than that of typical NPB based device. At 1000 cd $m^{-2}$, for example, fluorescent green OLED with NPVCz or DPPVCz layer demonstrate a $\eta_{CE}$ of 4.5 or 4.0 cd $A^{-1}$, which are almost 165 or 135% higher than that of typical HTM, NPB, based device. In addition, naphthalene substituted carbazole core type HTMs, NPVCz and DNPVCz, based devices also show a maximum luminance of 10360 cd $m^{-2}$ and 4748 cd $m^{-2}$, respectively, which are 146% and 13% higher than NPB based device. The reason why NPVCz and DNPVCz based devices show higher performance may be attributed to effective electrons and excitons confinement within the $Alq_3$ layer (EML/ETL), especially at high luminance, due to their low-lying LUMO energy levels.[9] Moreover, the high efficiency may attributed to smooth film morphology of NPVCz that can effectively prevent any undesirable current leakage throughout the device measurement. The resultant naphthyl substituted HTM, NPVCz, also exhibited relatively higher device performance than that of the phenyl substituted DPPVCz

counterpart (**Table 2**). In naphthalene substituted HTMs, we attribute the high device performance to the following factors, (i) relatively higher hole mobility than that of the phenyl substituted HTM, and (ii) matching HOMO energy levels that fascilitate injection of holes into the $Alq_3$ layer. All the four devices show an EL emission peak at 516 nm, which is directly correspond to the $Alq_3$ emission (**Fig. S10**).

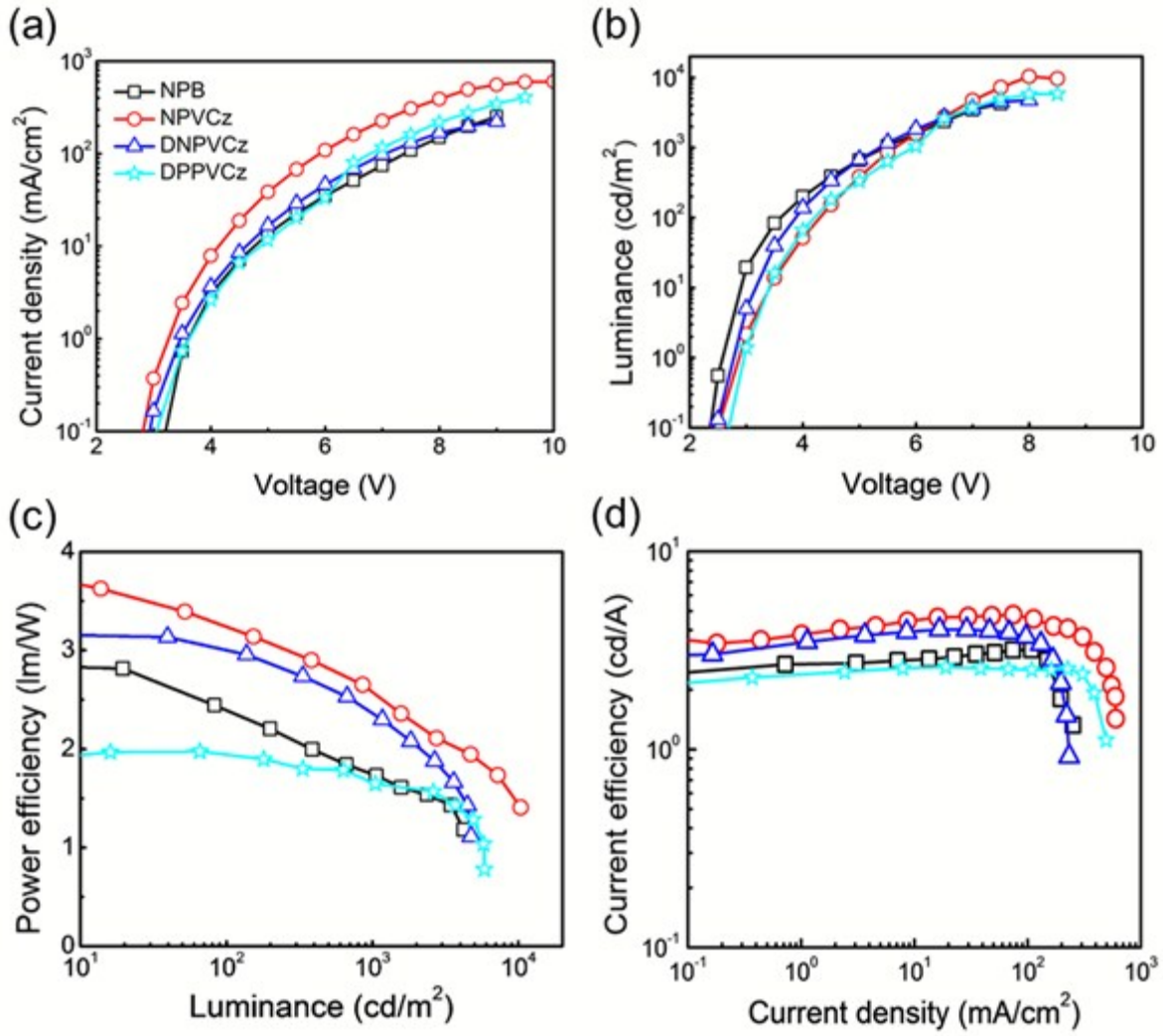


**Figure 6.** Effects of HTMs on the (a) current density, (b) luminance, (c) power efficiency vs luminance, and (d) current efficiency vs current density results of the fluorescent OLED devices.

### *2.6.2. Phosphorescent OLED devices*

**Table 3** shows the electroluminescent characteristics of conventional $Ir(ppy)_3$ based green phosphorescent devices with various HTMs, NPVCz, DNPVCz and DPPVCz, and NPB. The

View Article Online
DOI: 10.1039/C7TC03049E

NPB based control device shows a $\eta_{PE}$ of 30.6 lm $W^{-1}$ and a $\eta_{CE}$ of 41.4 cd $A^{-1}$, at 100 cd $m^{-2}$ (**Fig. S11**), which are almost 82% and 45% lower compared to the OLED devices based on the NPVCz. Moreover, the maximum $\eta_{CE}$ is markedly improved from 46.4 to 66.2 cd $A^{-1}$ (max. $\eta_{PE}$ from 48.5 to 70.0 lm $W^{-1}$, and a max. $\eta_{ext}$ from 14.2% to 18.3%). As shown in **Fig. 7**, the NPVCz containing device demonstrated a $\eta_{CE}$ of 60.1 cd $A^{-1}$ ($\eta_{PE}$ = 55.6 lm $W^{-1}$ and $\eta_{ext}$ = 17.1%), at 100 cd $m^{-2}$. On the contrary, DNPVCz containing device showed a $\eta_{CE}$ of 58.4 cd $A^{-1}$ ($\eta_{PE}$ = 54.8 lm $W^{-1}$ and $\eta_{ext}$ = 16.1%), while a 45.1 cd $A^{-1}$ ($\eta_{PE}$ = 40.8 lm $W^{-1}$ and $\eta_{ext}$ = 12.5%) for the DPPVCz containing device. The reason why the NPVCz based device showed the highest efficiencies among all the three studied HTMs may be attributed to three reasons, namely high hole mobility, appropriate HOMO and LUMO energy levels, and sufficiently high triplet energy.

**Table 3.** Effect of the carbazole based novel HTMs on the EL characteristics of phosphorescent OLED devices.

| HTL | $V_{driv.}$ (V) | $\eta_{PE}$ (lm/W) | $\eta_{CE}$ (cd/A) | $CIE_{x,y}$ coordinates | Maximum luminance ($cd/m^2$) |
|---|---|---|---|---|---|
| | @ 100 /1,000 $cd/m^2$ | | | | |
| NPB | 4.2/5.9 | 30.6/17.8 | 41.4/32.7 | (0.31, 0.63)/(0.31, 63) | 11560 |
| NPVCz | 3.5/4.6 | 55.6/34.3 | 60.1/50.2 | (0.31, 0.63)/(0.31, 63) | 15140 |
| DNPVCz | 3.4/4.7 | 54.8/26.6 | 58.4/39.8 | (0.30, 0.63)/(0.30, 63) | 9020 |
| DPPVCz | 3.5/4.7 | 40.8/24.5 | 45.1/36.1 | (0.31, 0.63)/(0.31, 63) | 12280 |

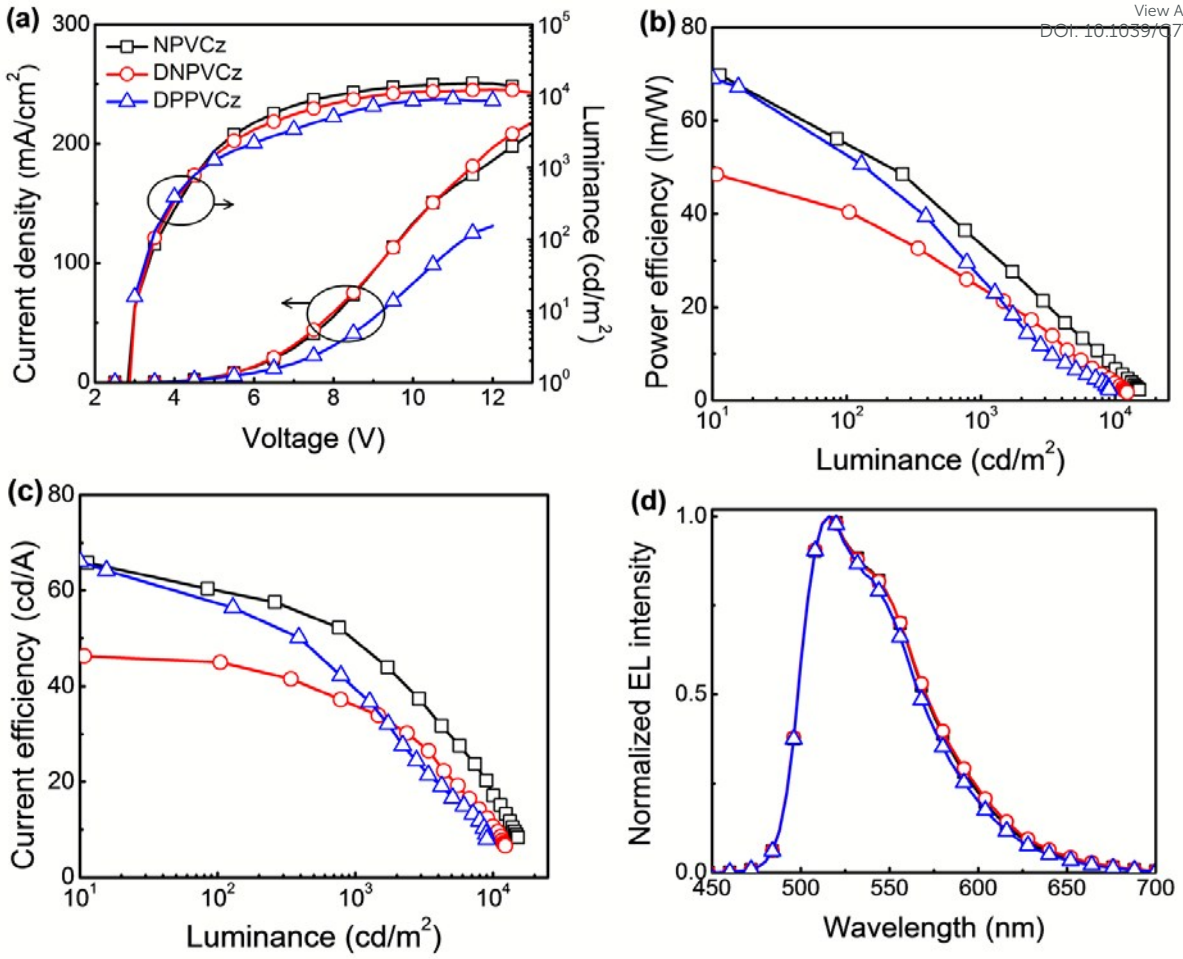


**Figure 7.** Effects of HTMs on the (a) current density and luminance, (b) power efficiency vs luminance, (c) current efficiency vs luminance, and (d) EL spectra of the phosphorescent OLED devices.

The NPVCz shows a highest hole mobility of $2.4 \times 10^{-4}$ $cm^2.V^{0.5}.s^{0.5}$, which is much higher than that of the DPPVCz and DNPVCz counterparts. The NPVCz favors an efficient hole injection in the device, and result a highest brightness among all four devices. Moreover, the resultant device architecture shows an energy barrier of 0.07 eV for hole to enter from HIL (PEDOT:PSS) and 0.33 or 0.73 eV to the $Ir(ppy)_3$ guest or CBP host. Whilst, the barrier is 0.11 eV for hole to enter from the HIL to the HTL DNPVCz and 0.29 or 0.69 eV further to the guest or host. The higher hole mobility and low energy barrier between the HIL and HTL may explain why device with NPVCz shows higher efficiencies.

The reason why the naphthyl substituted carbazole derivatives, NPVCz and DNPVCz, based devices exhibit relatively higher efficiency than that of phenyl substituted carbazole compound DPPVCz because of their higher $E_T$ values (**Table 1**). Moreover, all the three HTMs demonstrated a higher $E_T$ than that of the CBP host (2.6 eV). The resultant HTMs can effectively confine the electrons and excitons within the EML and result a bright emission with high efficiencies.[46]

As to DPPVCz, its resultant device structure shows an extremely high barrier for hole to enter into the guest or host, which in 0.67 or 1.07 eV. Although there is barely any barrier for the hole to enter from the HIL, the tremendously high barrier to further inject into the emissive layer is in a totally unfavorable position. This explains why the DPPVCz containing device shows lowest performance among all four devices studied. The NPVCz based device also show 54% and 92% higher in $\eta_{CE}$ and $\eta_{PE}$, respectively, compared to the conventional NPB based OLED (**Table 2** and **Fig. S11a** and **11b**). **Fig. 7d** and **Fig. 11c** show the EL spectra of devices that were collected at 100 and 1000 cd $m^{-2}$. The EL spectra of devices remained identical when naphthyl and phenyl substituted carbazole derivatives were utilized as the HTMs (**Fig. 7d**). Over the past years, numerous vinyl type compounds, such as PVK and VPEC, exhibit better hole transporting characteristics in the solution-processed devices than conventional aryl compounds, namely NPB and TPD.[15,21,25,40] The excellent performance of typical HTMs, PVK and VPEC, in solution-processed OLEDs motivated us to design molecular HTMs based on vinyl linkage.[47]

The operational lifetime ($t_{1/2}$), which is defined as a time when the luminance drops to 50% of initial luminance ($L_0$), of phosphorescent OLEDs was carried-out by operating the devices under a constant current with a varying initial brightness values at room temperature. **Fig. S12** shows the effect of HTMs, namely NPB, NPVCz, DNPVCz, and DPPVCz, on the device lifetime. The DNPVCz based device shows a lifetime of 1.63 h at the $L_0$ of 1914 cd $m^{-}$

$^{2}$, while conventional NPB based device exhibits a lifetime of 1.0 h at the $L_0$ of 2329 cd m$^{-2}$. The $t_{1/2}$ of DNPVCz device, at an initial brightness of 100 cd m$^{-2}$, can be extrapolated to 246 h. The devices with the NPVCz and DPPVCz HTMs also demonstrate the extrapolated $t_{1/2}$ of 160 h and 174 h, respectively, which are slightly lower than that of conventional NPB (208 h) counterpart. The DNPVCz shows a highest thermal degradation temperature among all the studied HTMs, NPVCz, DPPVCz, and NPB, that may also lead higher $t_{1/2}$ under the electrical excitation. Hence, it is worthy to investigate the degradation mechanism of vinyl linkage based molecular HTMs. The $t_{1/2}$ of solution-process OLEDs can be enhanced further by rationalizing the molecular design of naphthalene-substituted carbazole core based HTMs. These materials will open an avenue towards realization of high efficiency, long-lasting OLEDs for displays and lighting applications.

## 3. Conclusion

In conclusion we have designed and synthesized a series of naphthyl and phenyl substituted carbazole core based HTMs, NPVCz, DNPVCz, and DPPVCz, for high efficiency fluorescent and phosphorescent OLED devices. All the three molecular HTMs showed excellent solution-processability with much smooth film morphologies due to appropriate thermal stabilities and high solubility in common organic solvents. These HTMs, especially naphthyl derivatives NPVCz and DNPVCz, showed higher device efficiencies than that of typical NPB counterpart. Fluorescent device shows an improvement of 165% and 52%, in $\eta_{CE}$ and $\eta_{PE}$, respectively, as typical NPB is replaced with the NPVCz. The NPVCz based phosphorescent device showed a maximum $\eta_{PE}$ and $\eta_{CE}$ of 70.0 and 66.2 cd A$^{-1}$, respectively, and improves by over 40% compared to the OLED based on the NPB. The higher device performances are resulted because of rational hole transporting ability, smooth surface morphology, effective electron and exciton confinement function, and adequately high triplet energies. The naphthyl substituted carbazole derivatives can serve as potential molecular

View Article Online
DOI: 10.1039/C7TC03049E

HTMs in solution-processed OLED devices. These materials will open an avenue towards realization of high efficiency and long-lasting OLEDs for displays and lighting applications.

## 4. Experimental

### 4.1 Synthetic detail and spectral data

All the precursor compounds required for the synthesis were purchased from commercial sources and used as such without further purification. The 9*H*-carbazole (**1**), phenylacetaldehyde, (±)-camphor-10-sulfonic acid, 1-naphtalene boronic acid, phenyl boronic acid, bis(triphenylphosphine)palladium(II) dichloride ($Pd(PPh_3)_2Cl_2$), and potassium hydroxide were purchased from Aldrich and used as received without further purification. 3-Iodo-*9H*-carbazole (**2**) and 3,6-diiodo-*9H*-carbazole (**3**) were obtained by a procedure of Tucker.[40]

***3-Iodo-9-(2-phenylvinyl)carbazole*** (**4**): Firstly, 3-iodo-*9H*-carbazole (Compound **2**) (1.5 g, 5 mmol) was dissolved in toluene (15 ml) at 80 $^oC$. Subsequently, phenylacetaldehyde (1.32 ml, 11.3 mmol) was added dropwise into the stirred solution of Compound **2**. Then a (±)-camphor-10-sulfonic acid was added as a catalyst. The resultant mixture was stirred for 24 h at 110 $^oC$. Finally, the solvent was evaporated under vacuum and the resultant crude product was purified by silica gel column chromatography using hexane/diethyl ether (vol. ratio 30:1) as an eluent. The yield of Compound **4** was 0.56 g (50%).

$H^1$ NMR spectrum (300 MHz, $CDCl_3$, δ, ppm): 8.31 (d, 1H, J = 1.2 Hz, Ar); 7.95 (d, 1H, J = 7.2 Hz, Ar); 7.67 (dd, 1H, J1 = 1.5 Hz, J2 = 9.0 Hz, Ar); 7.63 (d, 1H, J = 8.7 Hz, Ar); 7.53 (d, 1H, J = 14.4 Hz, NCH=CHPh); 7.50 – 7.38 (m, 8H, Ar); 6.96 (d, 1H, J = 14.4 Hz, NCH=CHPh). IR (KBr, cm−1): 3057, 3022 (C-H in Ar); 1652 (C=C); 1616, 1599, 1574, 1468, 1442 (C=C in Ar); 1374, 1359, 1267, 1235, 1218 (C-N in Ar); 946 (=C-H trans); 871, 793, 743, 688 (C-H in Ar); 543, 506 (C-J). MS (APCI+, 20 V): 397.3 ([M+H], 100 %).

***3,6-Diiodo-9-(2-phenylvinyl)carbazole*** **(5)**: Firstly, a 3,6-di-iodo-9*H*-carbazole (Compound **3**) (8.7 g, 20.86 mmol) was dissolved in toluene (70 ml) at 80 $^{o}$C. Afterward, a phenylacetaldehyde (4.88 ml, 41.7 mmol) was added dropwise into the stirred solution of Compound **3**. Later, a (±)-camphor-10-sulfonic acid was added as catalyst. The solution was stirred for 24 h at 110 $^{o}$C. Finally, the solvent was evaporated under vacuum and the resultant crude product was purified by silica gel column chromatography using hexane/diethyl ether (vol. ratio 30:1) as an eluent. The yield of compound 7 was 8.1 g (75%).

$H^1$ NMR spectrum (400 MHz, $CDCl_3$, δ, ppm): 8.26 (d, 2H, J = 1.6 Hz, Ar); 7.71 (dd, 2H, J1 = 1.4 Hz, J2 = 8.7 Hz, Ar); 7.51 – 7.38 (m, 7H, Ar and NCH=CHPh); 7.32 (t, 1H, J = 6.9 Hz, Ar); 6.94 (d, 1H, J = 14.1 Hz, NCH=CHPh). IR (KBr, $cm^{-1}$): 3053, 3022 (C-H in Ar); 1650 (C=C trans); 1599, 1468, 1427 (C=C in Ar); 1367, 1357, 1284, 1234, 1216 (C-N in Ar); 923 (=C-H trans); 803, 793, 743,689 (C-H in Ar); 564, 558, 507 (C-J). MS (APCI+, 20 V): 522.2 ([M+H], 100 %).

***3-(1-Naphthyl)-9-(2-phenylvinyl)carbazole*** **(NPVCz)**: In order to synthesize the target compound NPVCz, a 0.3 g (0.75 mmol) of 3-iodo-9-(2-phenylvinyl)carbazole (Compound **4**), a 0.26 g (1.51 mmol) of 1-naphtalene boronic acid, a 0.023 g (0.033 mmol) of $PdCl_2(PPh_3)_2$, and a 0.21 g (3.7 mmol) of powdered potassium hydroxide were dissolved in 5 ml of THF solvent. Then the resultant mixture was stirred for 24 h at 80 $^{o}$C under nitrogen atmosphere. Subsequently, the reaction mixture was cooled and then quenched in an ice bath. The resultant compound was extracted by using a chloroform solvent. The extract was dried by using an anhydrous $Na_2SO_4$. Finally, the resultant extract was purified by silica gel column chromatography using a mixture of ethyl acetate and hexane (vol. ratio 1:50) as an eluent. Yield: 0.25 g (83%) of white crystals.

View Article Online
DOI: 10.1039/C7TC03049E



$H^1$ NMR spectrum (400 MHz, $CDCl_3$, δ, ppm): 8.19 (d, 1H, J = 1.2 Hz, Ar); 8.07 (d, 1H, J = 7.2 Hz, Ar); 8.00 (d, 1H, J = 8.4 Hz, Ar); 7.92 (d, 1H, J = 8.0 Hz, Ar); 7.88 (dd, 1H, J1 = 1.8 Hz, J2 = 7.6 Hz, Ar); 7.82 (d, 1H, J = 8.0 Hz, Ar); 7.75 (d, 1H, J = 14.4 Hz, NCH=CHPh); 7.70 (d, 1H, J = 8.0 Hz, Ar); 7.62 (dd, 1H, J1 = 2.0 Hz, J2 = 8.4 Hz, Ar); 7.58 -7.39 (m, 9H, Ar); 7.34 – 7.28 (m, 2H, Ar); 7.12 (d, 1H, J = 14.4 Hz, NCH=CHPh). IR (KBr, cm−1): 3053 (C-H in Ar); 1648 (C=C); 1622, 1600, 1565, 1486, 1455 (C=C in Ar); 1395 (naphthyl group); 1375, 1331, 1236 (C-N in Ar); 939 (=C-H trans); 889, 819, 776, 746 (C-H in Ar). MS (APCI+, 20 V): 396.4 ([M+H], 100 %).

***3,6-Di-(1-Naphthyl)-9-phenylvinylcarbazole*** **(DNPVCz)**: In order to synthesize the target compound DNPVCz, a 1.0 g (1.92 mmol) of 3,6-diiodo-9-(2-phenylvinyl)carbazole (5), a 0.68 g (5.76 mmol) of 1-naphtalene boronic acid, a 0.081 g (0.12 mmol) of $PdCl_2(PPh_3)_2$ and a 1.08 g (19.25 mmol) of powdered potassium hydroxide were dissolved in 15 ml of a THF solvent. The resultant mixture was stirred for 24 h at 80 $^oC$ under nitrogen atmosphere. Subsequently, the reaction mixture was cooled and quenched in an ice bath. Then the product was extracted by a chloroform solvent. The resultant extract was dried by using an anhydrous $Na_2SO_4$. Finally, the extract was purified by silica gel column chromatography using a mixture of ethyl acetate and hexane (vol. ratio 1:20) as an eluent. Yield: 0.5 g (50%) of white crystals.

$H^1$ NMR spectrum (400 MHz, $CDCl_3$, δ, ppm): 8.13 (dd, 2H, J1 = 1.6 Hz, J2 = 7.2 Hz, Ar); 8.04 (d, 2H, J = 0.8 Hz, Ar); 7.73 (dd, 2H, J1 = 2.4 Hz, J2 = 7.2 Hz, Ar); 7.69 (d, 2H, J = 8.4 Hz, Ar); 7.54 (dd, 2H, J1 = 1.6 Hz, J2 = 8.4 Hz, Ar); 7.51 – 7.45 (m, 5H, Ar and NCH=CHPh)); 7.38 (tr, 2H, J = 7.6 Hz, Ar); 7.32 -7.26 (m, 6H, Ar); 7.23 (tr, 2H, J = 7.6 Hz, Ar); 7.13 (tr, 1H, J = 7.2 Hz, Ar); 7.12 (d, 1H, J = 14.4 Hz, NCH=CHPh). IR (KBr, $cm^{-1}$): 3036 (C-H in Ar); 1650 (C=C); 1626, 1488, 1470, 1453 (C=C in Ar); 1392 (naphthyl group);

1357 (C-N in Ar); 939 (=C-H trans); 882, 811, 800, 778, 690 (C-H in Ar). MS (APCI+, 20 V): 522.7 ([M+H], 100 %).

***3,6-Diphenyl-9-(2-phenylvinyl)carbazole*** **(DPPVCz)**: In order to synthesize the target compound DPPVCz, a 1.5 g (2.9 mmol) of 3,6-diiodo-9-(2-phenylvinyl)carbazole (5), a 1.05 g (8.6 mmol) of phenyl boronic acid, a 0.12 g (0.17 mmol) of $PdCl_2(PPh_3)_2$, and a 1.6 g (28.5 mmol) of powdered potassium hydroxide were dissolved in 20 ml of a THF solvent. The resultant mixture was stirred for 24 h at 80 $^oC$ under nitrogen atmosphere. Then the reaction mixture was cooled and quenched by the addition of ice water. Finally, the quenched reaction mixture was extracted by chloroform after that the resultant extract was dried by using the anhydrous $Na_2SO_4$. The dry extract was purified by silica gel column chromatography using the mixture of ethyl acetate and hexane (vol. ratio 1:40) as an eluent. Yield: 0.22 g (18%) g of white crystals.

$H^1$ NMR spectrum (300 MHz, $CDCl_3$, δ, ppm): 8.18 (d, 2H, J = 1.8 Hz, Ha); 7.74 – 7.26 (m, 20H, Ar); 7.10 (d, 1H, J = 14.8 Hz, NCH=CHPh). IR (KBr, $cm^{-1}$): 3057, 3028 (C-H in Ar); 1649 (C=C); 1625, 1598, 1475, 1456 (C=C in Ar); 1373, 1363, 1227 (C-N in Ar); 934, 925, 875, 868, 761, 696 (C-H in Ar). MS (APCI+, 20 V): 422.6 ([M+H], 100 %).

### 4.2 Materials and characterization

The indium tin oxide (ITO) coated glass substrates with a sheet resistance of 15 Ω/□ and a light transmittance greater than 84% were purchased from Luminescence Technology Corporation. The hole injection material poly(3,4-ethylene-dioxythiophene)-poly(styrenesulfonate) (PEDOT:PSS) with a purity of 99.9% was purchased from Bayer Taiwan. The electron transporting material TPBi was purchased from e-Ray Optoelectronic. Typical fluorescent and phosphorescent green emitters, respectively, $Alq_3$ and *tris*(2-phenyl-pyridine) iridium $(Ir(ppy)_3$ were purchased from Luminescence Technology Corporation.

View Article Online
DOI: 10.1039/C7TC03049E

Lithium fluoride (LiF) (purity 99.95%) was purchased from Strem Chemicals Corporation. Aluminum (Al) ingots (99.999%) were purchased from Showa Chemical Co. Ltd. All the materials were used without further purification.

Column chromatography purifications were performed with silica gel (70-230 mesh) as a stationary phase in a column with 50 cm long and 5 cm diameter. $^1$H NMR spectra were recorded using a Varian Unity Inova (300 MHz) apparatus. Mass spectra of the compounds were obtained on a Waters ZQ 2000 spectrometer in the positive ion mode. The PL spectra of the compounds were recorded in THF at room temperature in quartz cuvettes using a Fluorolog III photoluminescence spectrometer. The UV-vis spectra of the compounds were recorded in THF at room temperature using a UV-Vis spectrophotometer.

Cyclic voltammetry (CV) experiments were performed in an electrochemical workstation using a three electrode assembly comprising glassy carbon working electrode, a non-aqueous Ag/AgCl reference electrode, and an auxiliary platinum electrode. The experiments were performed at room temperature under nitrogen atmosphere in dichloromethane using a 0.1 M tetrabutylammonium perchlorate ($Bu_4NClO_4$) as supporting electrolyte on a CH-instruments CH1604A potentiostat. The $E_{1/2}^{ox}$ values were determined using $(E_p^a + E_p^c)/2$, where $E_p^a$ and $E_p^c$ are the anodic and cathodic peak potentials, respectively.

Differential scanning calorimetry (DSC) measurements were carried out using a Bruker Reflex II thermosystem. Thermogravimetric analysis (TGA) was performed using a Netzsch STA 409 apparatus. The DSC and TGA curves were recorded in a nitrogen atmosphere at a ramp rate of 10 $^o$C min.$^{-1}$.

### 4.3 Device fabrication and characterization

View Article Online
DOI: 10.1039/C7TC03049E



**Fig. 5** shows the schematic energy-level diagrams of the OLED devices studied herein. Taking the fluorescent green OLED device for example, the fabrication process included firstly spin-coating an aqueous solution of PEDOT:PSS at 4,000 rpm for 20 s to form a hole-injection layer (HIL) on a pre-cleaned ITO anode. Before spin-coating the following hole transporting layer (HTL), the solution was prepared by dissolving 4 mg $ml^{-1}$ of the HTMs (NPVCz, DNPVCz, DPPVCz, and NPB) in tetrahydrofuran at room-temperature with stirring for 0.5 h. The resulting solution was then spin-coated at 2,500 rpm for 20 s under nitrogen. Followed were the depositions of the emission layer/electron-transporting layer $Alq_3$, the electron injection layer LiF, and the cathode Al, by thermal evaporation in a vacuum chamber at a vacuum level of less than $5 \times 10^{-6}$ Torr.

For phosphorescent green device, a 32 nm HIL of PEDOT:PSS was spin-coated on a pre-cleaned ITO coated glass substrates. Subsequently, molecular HTMs (NPVCz, DNPVCz, DPPVCz and NPB) were spin-coated on the PEDOT:PSS coated substrates and a 20 nm EML (10 wt% $Ir(ppy)_3$ doped in the CBP host) was deposited on the annealed HTL via spin-coating method (2000 rpm for 30 s). Later on, a 35 nm ETL of TPBi and a 1 nm EIL of LiF were thermally-evaporated with 0.5 Å $s^{-1}$ and 0.1 Å $s^{-1}$. Finally, a 100 nm Al cathode layer was deposited by the thermal-evaporation.

The luminance, CIE chromatic coordinates, and electroluminescent spectrum of the resultant green OLEDs were measured by using a Photo Research PR-655 spectrascan and CS100A luminance meter. A Keithley 2400 source meter was used to measure the current-voltage (*I–V*) characteristics. The emission area of the devices was 25 $mm^2$, which is defined by the overlapping area between anode and cathode layers, and only the luminance in the forward direction was measured.

## Acknowledgement

View Article Online
DOI: 10.1039/C7TC03049E

This work was financially supported by Ministry of Science and Technology through the grant numbers of 100-2119-M-007-011-MY3 and 103-2923-E-007-003-MY3, Ministry of Economic Affairs through the grant number MEA 102-EC-17-A-07-S1-181, and by Research Council of Lithuania (grant No. TAPLLT1/14).

## Declaration

There are no conflicts of interest to declare.

## References

1 F. So, J. Kido, and P. Burrows, *MRS Bull.*, 2008, **33**, 663.

2 B. W. D'Andrade, S. R. Forrest, *Adv. Mater.*, 2004, 16, 1585.

3 S. R. Forrest, Nature, 2004, **428**, 911.

4 H. Kim, Y. Byun, R. R. Das, B. K. Choi, and P. S. Ahn, *Appl. Phys. Lett.*, 2007, **91**, 093512.

5 T.-W. Lee, T. Noh, H.-W. Shin, O. Kwon, J.-J. Park, B.-K. Choi, M.-S. Kim, D. W. Shin, and Y.-R. Kim, *Adv. Mater.*, 2009, **19**, 1625.

6 J.-H. Jou, M.-F. Hsu, W.-B. Wang, C.-L. Chin, Y.-C. Chung, C.-T. Chen, J.-J. Shyue, S.-M. Shen, M.-H. Wu, W.-C. Chang, C.-P. Liu, S.-Z. Chen and H.-Y. Chen, *Chem. Mater.*, 2009, **21**, 2565.

7 J.-H. Jou, Y.-M. Yang, S.-Z. Chen, J.-R. Tseng, S.-H. Peng, C.-Y. Hsieh, Y.-X. Lin, C.-L. Chin, J.-J. Shyue, S.-S. Sun, C.-T. Chen, C.-W. Wang, C.-C. Chen, S.-H. Lai and F.-C. Tung, *Adv. Optical Mater.*, 2013, **1**, 657.

8 J.-H. Jou, Y.-X. Lin, S.-H. Peng, C.-J. Li, Y.-M. Yang, C.-L. Chih, J.-J. Shyue, S.-S. Sun, M. Lee, C.-T. Chen, M.-C. Liu, C.-C. Chen, G.-Y. Chen, J.-H. Wu, C.-H. Li, C.-F. Sung, M.-J. Lee, and J.-P. Hu, *Adv. Funct. Mater.*, 2014, **24**, 555.

9 J.-H. Jou, S. Kumar, P.-H. Fang, A. Venkateswararao, K. R. J. Thomas, J.-J. Shyue, Y.-C. Wang, T.-H. Li, and H.-H Yu, *J. Mater. Chem. C*, 2015, **3**, 2182.

10 C. Adachi, T. Tsutsui and S. Saito, *Appl. Phys. Lett.*, 1990, **57**, 531.

11 D. O'Brien, A. Bleyer and D. G. Lidzey, *J. Appl. Phys.*, 1997, **82**, 2662.

12 J. H. Jou, S. Kumar, A. Agrawal, T.-H. Li, and S. Sahoo, *J. Mater. Chem. C*, 2015, **3**, 2974.

13 C. Adachi, K. Nagai and N. Tamoto, *Appl. Phys. Lett.*, 1995, **66**, 2679.

14 B. E. Koene, D. E. Loy and M. E. Thompson, *Chem. Mater.*, 1998, **10**, 2235.

15 Q. Huang, G. A. Evmenenko, P. Dutta, P. Lee, N. R. Armstrong and T. J. Marks, *J. Am. Chem. Soc.*, 2005, **127**, 10227.

16 S. H. Kim, J. Jang, and J. Y. Lee, *Appl. Phys. Lett.*, 2007, **90**, 223505.

17 S. O. Jeon, K. S. Yook, C. W. Joo, J. Y. Lee, K. Y. Ko, J. Y. Park, and Y. G. Baek, *Appl. Phys. Lett.*, 2008, **93**, 063306.

18 R. J. Holmes, S.R. Forrest, R.C. Kwong, J.J. Brown, S. Garon, and M.E. Thompson, *Appl. Phys. Lett.*, 2003, **82**, 2422.

19 M. Ikai, S. Tokito, Y. Sakamoto, T. Suzuki, and Y. Taga, *Appl. Phys. Lett.*, 2001, **79**, 156.

20 J. Lee, N. Chopra, S. H. Eom, Y. Zheng, J. Xue, and F. So, J. Shi, *Appl. Phys. Lett.*, 2008, **93**, 123306.

21 L. H. Chan, R. H. Lee, C. F. Hsieh, H. C. Yeh and C. T. Chen, *J. Am. Chem. Soc.*, 2002, **124**, 6469.

22 P. M. Borsenberger, E. H. Magin, and J. J. Fitzgerald, *J. Phys. Chem.*, 1993, **97**, 8250.

23 S. Tokito, H. Tanaka, A. Okada, and Y. Taga, *Appl. Phys. Lett.* 1996, **69**, 878.

24 Y. Kuwabara, H. Ogawa, H. Inada, N. Noma, and Y. Shirota, *Adv. Mater*., 1994, **6**, 677.

25 J.-H. Jou, T.-H. Li, S. Kumar, C.-C. An, A. Agrawal, S.-Z. Chen, P.-H. Fang, G. Krucaite, S. Grigalevicius, J. Grazulevicius, and C.-F. Sung, *Org. Electron.*, 2015, **24**, 254.

26 Y. H. Niu, M. S. Liu, J. W. Ka, J. Bardeker, M. T. Zin, R. Schofield, Y. Chi, and A. K.Y. Jen, *Adv. Mater.*, 2007, **19**, 300.

27 Z. Jiang, T. Ye, C. Yang, D. Yang, M. Zhu, C. Zhong, J. Qin, and D. Ma, *Chem. Mater.*, 2011, **23**, 771.

28 C. Zhong, C. Duan, F. Huang, H. Wu, and Y. Cao, *Chem. Mater.*, 2011, **23**, 326.

29 Y.-J. Cheng, M. S. Liu, Y. Zhang, Y.-H. Niu, F. Huang, J.-W. Ka, H.-L. Yip, and A. K.-Y. Jen. *Chem. Mater.* 2008, **20**, 413.

30 P. Zacharias, M. C. Gather, M. Rojahn, O. Nuyken, and K. Meerholz, *Angew. Chem., Int. Ed.* 2007, **46**, 4388.

31 B. Domercq, R. D. Hreha, Y.-D. Zhang, N. Larribeau, J. N. Haddock, C. Schultz, S. R. Marder, and B. Kippelen, *Chem. Mater.* 2003, **15**, 1491.

32 I. K. Yakushchenko, M. G. Kaplunov, O. N. Efimov, M. Y. Belov, and S. N. Shamaev, *Phys. Chem. Chem. Phys.*, 1999, **1**, 1783.

33 P. Moonsin, N. Prachumrak, R. Rattanawan, T. Keawin, S. Jungsuttiwong, T. Sudyoadsuk, and V. Promarak, *Chem. Commun.*, 2012, **48**, 3382.

34 O. Usluer, S. Demic, D. A. M. Egbe, E. Brickner, C. Tozlu, A. Privrikas, A. M. Ramil, and N. S. Sariciftci, *Adv. Funct. Mater.* 2010, **20**, 4152.

35 N. Prachumrak, S. Pansay, S. Namuangruk, T. Kaewin, S. Jungsuttiwong, T. Sudyoadsuk, and V. Promarak, *Eur. J. Org. Chem.* 2013, **2013**, 6619.

36 T. Tsuboi, S.-W. Liu, M.-F. Wu, and C.-T. Chen, *Org. Electron.* 2009, **10**, 1372.

37 L. Duan, L. Hou, T.-W. Lee, J. Qiao, D. Zhang, G. Dong, L. Wang, and Y. Qiu, *J. Mater. Chem.* 2010, **20**, 6392.

38 C. S. Wu, S. W. Fang, and Y. Chen, *Phys. Chem. Chem. Phys.*, 2013, **15**, 15121.

39 A. M. Thaengthong, S. Seangsuwan, S. Jungsuttiwong, T. Keawin, T. Sudyoadsuk, and V. Promarak, *Tetrahedron Lett.*, 2011, **52**, 4749.

40 H. Tucker, *J. Chem. Soc.* 1926, **1**, 548.

41 (a) J.-H. Jou, W.-B. Wang, S.-M. Shen, S. Kumar, I.-M. Lai, J.-J. Shyue, S. Lengvinaite, R. Zostautiene, J. V. Grazulevicius, S. Grigalevicius, S.-Z. Chen and C.-C. Wu, *J. Mater. Chem.*, 2011, **21**, 9546. (b) W. J. Shen, R. Dodda, C. C. Wu, F. I. Wu, T. H. Liu, H. H. Chen, C. H. Chen and C. F. Shu, *Chem. Mater.*, 2004, 16, 930. (c) H. Doi, M. Kinoshita, K. Okumoto and Y. Shirota, *Chem. Mater.*, 2003, 15, 1080. (d) J.-H. Jou, S. Sahoo, S. Kumar, H.-H. Yu, P.-H. Fang, M. Singh, G. Krucaite, D. Volyniuk, J. V. Grazulevicius, S. Grigalevicius, *J. Mater. Chem.C*, 2015, **3**, 12297.

42 C. A. Amorim, M. R. Cavallari, G. Santos, F.J. Fonseca, A. M. Andrade, and S. Mergulhao, *J. Non-Cryst. Solids*, 2012, **358**, 484.

43 S. C. Tse, C. H. Cheung, S. K. So, in: F. So (Ed.), Organic Electronics Materials, Processing, Devices and Applications, *Taylor & Francis*, London, 2010, pp. 71-74. Chapter 3.

44 W. Y. Hung, L. C. Chi, W. J. Chen, Y. M. Chen, S. H. Chou, K. T. Wong, *J. Mater. Chem.*, 2010, **20**, 10113.

45 M. H. Tsai, T. H. Ke, H. W. Lin, C. C. Wu, S. F. Chiu, F. C. Fang, Y. L. Liao, K. T. Wong, Y. H. Chen, C. I. Wu, *ACS Appl. Mater. Interfaces*, 2009, **1**, 567.

46 J. Lee, N. Chopra, S.-H. Eom, Y. Zheng, J. Xue, F. So, and J. Shi, *Appl. Phys. Lett.* 93, 123306, 2008.

47 R.-Q. Png, P.-J. Chia, J.-C. Tang, B. Liu, S. Sivaramakrishnan, M. Zhou, S.-H. Khong, H. S. O. Chan, J. H. Burroughes, L.-L. Chua, R. H. Friend, P. K. H. Ho, *Nat. Mater.* **2010**, *9*, 152.